Comparison of relativistic and nonrelativistic approaches to the collective model treatment of $p + {}^{40}$Ca inelastic scattering

S. Shim, B. C. Clark, E. D. Cooper, and S. Hama
Department of Physics, The Ohio State University, Columbus, Ohio 43210

R. L. Mercer
Thomas J. Watson Research Center, International Business Machines Corp., Yorktown Heights, New York 10598

L. Ray
Department of Physics, University of Texas, Austin, Austin, Texas 78712

J. Raynal
Service de Physique Théorique, Centre d'Etudes Nucléaires, Saclay, F- 91191, Guf-sur-Yvette CEDEX, France

H. S. Sherif
Nuclear Research Centre, University of Alberta, Edmonton, Alberta, Canada T6G 2N5
(Received 23 May 1990)

Elastic and inelastic observables for the scattering of 500 MeV protons from ^{40}Ca are calculated using either the first-order relativistic or nonrelativistic impulse approximation for the diagonal potentials and a collective model for the transition potentials. The calculations are done using either Dirac or Schrödinger coupled channel programs. The relativistic approach reproduces the inelastic observables better than the first-order nonrelativistic impulse approximation model.

I. INTRODUCTION

We have previously shown[1] that a simple collective model based on the relativistic impulse approximation[2-5] (RIA) could successfully reproduce elastic and inelastic $p + {}^{40}$Ca observables at 500 MeV. In this paper we compare the results of that relativistic calculation with a similar collective model based on the first order nonrelativistic impulse approximation of Kerman, McManus, and Thaler (KMT).[4,6,7] We use as far as possible expressions for the RIA and KMT optical potentials that contain the same physics. For example, no medium effects are included in either case, and the calculations are done in the local "$t\rho$" approximation. This simple approach, in our view, allows more direct comparison between the two model calculations.

In our earlier work[1] the diagonal Lorentz scalar and vector potentials were calculated using the approach given in Ref. 3. The input to the calculation consists of the SP88 *NN* amplitudes of Arndt[8] expressed in a Lorentz covariant form as in Ref. 9 and relativistic mean field densities of Horowitz and Serot.[10] A simple collective model was used in determining the transition potentials which were either taken to be proportional to the derivatives of the diagonal RIA potentials or obtained from folding the derivatives of the densities with the invariant *NN* amplitudes. The differences in the two approaches were slight and in this work we consider only the first procedure. The parameters in the collective model are the scalar and vector deformation lengths δ_s and δ_v, which were chosen to fit the inelastic cross section and analyzing power data. The RIA tensor was not included as its effect on elastic and inelastic observables at 500 MeV was slight.[11] The analysis showed that the RIA based calculation could successfully reproduce the inelastic observables for the low lying collective states, and that the inclusion of these states within the coupled channel formalism produced considerable improvement in the agreement with large angle elastic data. Similar results have also been obtained using purely phenomenological direct potentials as the input to the collective model calculations.[12]

In this work we consider the same experimental data treated using the nonrelativistic KMT approach described in Ref. 4 for the diagonal potentials and calculate the transition potentials using the collective model. In so far as possible the input for the RIA and KMT calculations are identical, the SP89 *NN* amplitudes are used in both. In the relativistic calculations the scalar and vector densities of Ref. 10 were used; only the vector densities are used in the KMT calculations. The central and spin-orbit KMT optical potentials are deformed to give the transition potentials. Full deformed spin-orbit coupling was included. Different deformation lengths, δ_c and $\delta_{s.o.}$, could be used in general for the real and imaginary parts of the transition potentials for a maximum of four parameters, the same number as in the RIA. The KMT optical potentials were input to a set of coupled Schrödinger equations and the deformation parameters were determined by fitting the inelastic data. Relativistic kinematics were used in the calculations.

We consider three questions. First, how do the first-

order KMT and RIA coupled channel predictions for the large angle elastic scattering compare with each other and with the data? Second, how well does the KMT based model describe the low-lying collective states of ^{40}Ca? Third, are differences between the RIA and KMT inelastic results due solely to the use of the coupled channel Dirac equations rather than the coupled Schrödinger equations?

In the next section we briefly describe the collective model results and in Sec. III we give our conclusions.

II. RESULTS OF THE COLLECTIVE MODEL CALCULATION

The RIA Lorentz scalar and vector (time-like) optical potentials are written

$$U_S(r)=-\frac{P_{\rm lab}}{4\pi^2 m}\sum_{i=p,n}\int d^3q\, e^{-i\mathbf{q}\cdot\mathbf{r}}\frac{R(q)}{R(0)}F_S^{(i)}(q)\times\int d^3r' e^{i\mathbf{q}\cdot\mathbf{r}'}\rho_S^{(i)}(r')\,, \quad (1)$$

$$U_V(r))=-\frac{P_{\rm lab}}{4\pi^2 m}\sum_{i=p,n}\int d^3q\, e^{-i\mathbf{q}\cdot\mathbf{r}}\frac{R(q)}{R(0)}F_V^{(i)}(q)\times\int d^3r' e^{i\mathbf{q}\cdot\mathbf{r}'}\rho_V^{(i)}(r')\,, \quad (2)$$

where the subscripts S and V refer to scalar or vector quantities, the superscripts n and p refer to neutrons and protons, $P_{\rm lab}$ is the laboratory momentum for the incident proton, $R(q)$ is the kinematical factor required to obtain the NN amplitude in the Breit frame as defined in Eq. (B3b) in Appendix B of Ref. 4, $F(q)$ is the invariant NN scattering amplitude, and m is the mass of the proton. The corresponding transition potentials between the ground state and the excited state with quantum numbers λ and μ are given by,

$$U_S^{\lambda,\mu}(\mathbf{r})=-\frac{\delta_s^\lambda}{(2\lambda+1)^{1/2}}\frac{dU_S(r)}{dr}Y^*_{\lambda\mu}(\Omega)\,, \quad (3)$$

$$U_V^{\lambda,\mu}(\mathbf{r})=-\frac{\delta_v^\lambda}{(2\lambda+1)^{1/2}}\frac{dU_V(r)}{dr}Y^*_{\lambda\mu}(\Omega)\,, \quad (4)$$

where λ refers to the multipolarity of the transition and δ_s^λ and δ_v^λ are the scalar and vector deformation lengths. These potentials are input to a set of coupled Dirac equations.[11–13] In the calculation the static Coulomb potential is obtained from the empirical charge distribution. We do not include the anomalous magnetic moment term nor the corresponding electromagnetic spin-orbit potential term in the KMT calculations. Both terms are insignificant for this case.[14]

The first order KMT potentials are given by[4]

$$U_C(r)=\frac{A-1}{A}\frac{1}{(2\pi)^3}\sum_{i=p,n}\int d^3q\, e^{-i\mathbf{q}\cdot\mathbf{r}}t_c^{(i)}(q)\int d^3r' e^{i\mathbf{q}\cdot\mathbf{r}'}\rho^{(i)}(r')\,, \quad (5)$$

$$U_{\rm s.o.}(r)=\frac{A-1}{A}\frac{1}{(2\pi)^3}\sum_{i=p,n}\frac{id}{r\,dr}\int d^3q\, e^{-i\mathbf{q}\cdot\mathbf{r}}\frac{t_{\rm s.o.}^{(i)}(q)}{k^2\sin\theta}\int d^3r' e^{i\mathbf{q}\cdot\mathbf{r}'}\rho^{(i)}(r') \equiv\frac{1}{r}\frac{d}{dr}V_{\rm s.o.}(r)\,. \quad (6)$$

Here A is the number of nucleons in the target, t_c and $t_{\rm s.o.}$ are the central and spin-orbit NN amplitudes in the Breit frame obtained from the SP89 Arndt amplitudes, k is the proton-nucleus c.m. momentum and θ is defined by $q=2k\sin(\theta/2)$; q is the momentum transfer. The central and spin-orbit transition potentials between the ground state and the excited state with quantum numbers λ and μ are written[15]

$$U_C^{\lambda,\mu}(\mathbf{r})=-\frac{\delta_c^\lambda}{(2\lambda+1)^{1/2}}\frac{dU_C(r)}{dr}Y^*_{\lambda\mu}(\Omega)\,, \quad (7)$$

$$U_{\rm s.o.}^{\lambda,\mu}(\mathbf{r})=-\frac{\delta_{\rm s.o.}^\lambda}{(2\lambda+1)^{1/2}}\sigma\cdot\left[\nabla\left[\frac{dV_{\rm s.o.}(r)}{dr}Y^*_{\lambda\mu}(\Omega)\right]\times\frac{1}{i}\nabla\right]\,, \quad (8)$$

where λ is the multipolarity of the transition. These diagonal and transition optical potentials are used in a set of coupled Schrödinger equations.[16]

The computer code ECIS87[17] was used for both computations. Checks were made using the Dirac coupled channel code CENITH,[13] the Dirac elastic scattering code RUNT[18] and the Schrödinger elastic scattering code KMT-80.[19]

The collective model described here, can accommodate from one to four free parameters, for either RIA or KMT based calculations. For example, the observables shown in Figs. 1–4, were calculated with $\delta_s=\delta_v$ and $\delta_c=\delta_{\rm s.o.}$ so that only one parameter remained in the search. For the RIA model we found that almost equivalent fits (in the chi-square sense), to the inelastic data could be obtained using one, two (real and imaginary deformation lengths taken equal), three, or four free parameters. However, we point out that when more than three parameters are used there is considerable ambiguity in the results. For example, the extracted δ's from the four parameter fit can differ from the two parameter results by an order of magnitude. This clearly indicates that one should restrict the number of parameters if they are to be given any physical

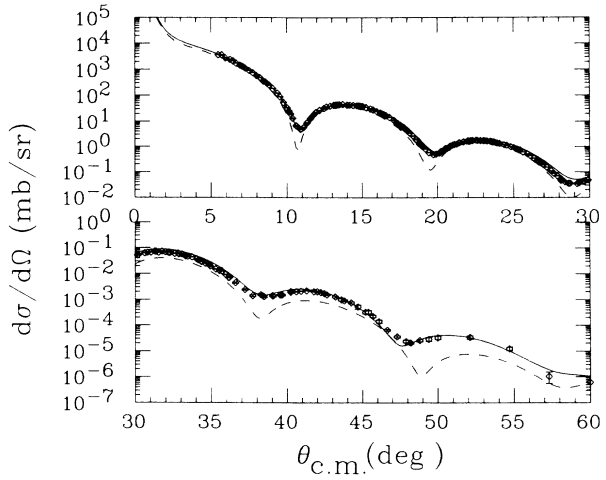

FIG. 1. RIA (solid line) and KMT (dashed line) elastic cross sections for $p+^{40}$Ca at 497.5 MeV. The 3^- state is included. The data are from Ref. 20.

interpretation. In order to appreciate the origin of this ambiguity, consider a DWBA calculation. Since the overall phase of the T matrix is not observable one can see that it is possible to obtain at most three parameters from the search. Even for the three parameter situation there exist ambiguities regarding which three parameters are being included in the search. In view of this, we present results for one and two parameter searches only. In fact, we found that the addition of one more parameter did not improve the fit. In the searches discussed in this work only one excited state was coupled to the elastic channel at a time.

In the KMT calculation, increasing the number of free parameters from one to four did not produce agreement with the inelastic spin observables although the chi-square per degree of freedom was decreased. The inability of this model to give good agreement with the inelastic

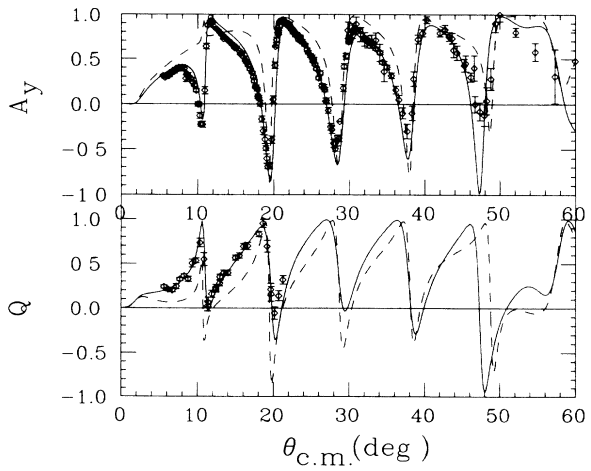

FIG. 2. The analyzing power and spin rotation function for the two cases shown in Fig. 1.

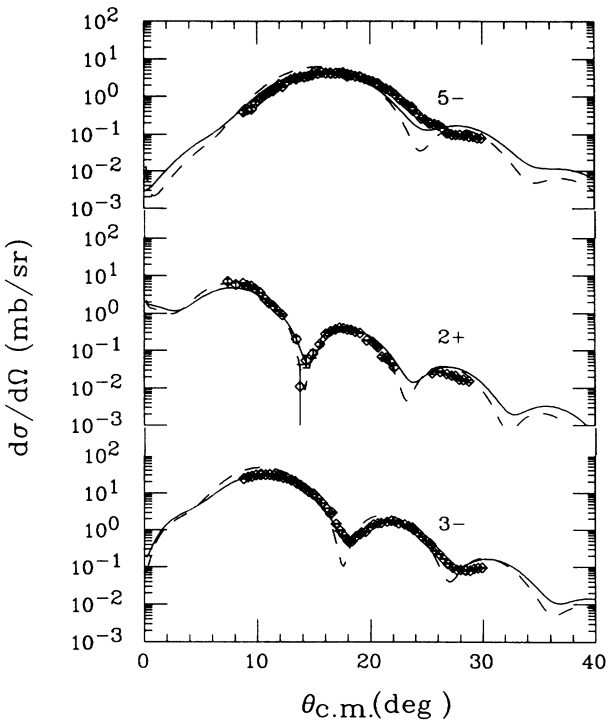

FIG. 3. Calculated inelastic ^{40}Ca(p,p') cross sections for the 2^+, 3^-, and 5^- states using RIA (solid line) and KMT (dashed line) optical potentials in the calculation. The data are from Refs. 21 and 22.

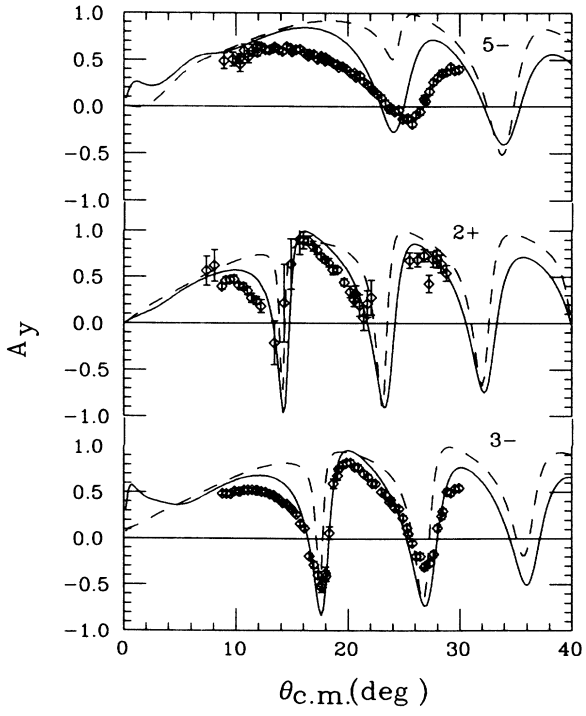

FIG. 4. Calculated analyzing powers for the states shown in Fig. 3. The data are from Refs. 21 and 22.

TABLE I. The deformation lengths determined from the one parameter fits to the 497.5 MeV ^{40}Ca(p,p') data. The KMT, RIA, or RIA-SE optical potentials were used in the collective model calculations.

State		δ (fm)	$\frac{\chi^2_{e,CS}}{N}$	$\frac{\chi^2_{e,Ay}}{N}$	$\frac{\chi^2_{e,Q}}{N}$	$\frac{\chi^2_{i,CS}}{N}$	$\frac{\chi^2_{i,Ay}}{N}$
3^-	δ_{KMT}	1.756	764	263	73	546	209
(3.74 MeV)	δ_{RIA}	1.352	91	48	5	60	49
	$\delta_{RIA\text{-}SE}$	1.318	94	69	10	56	45
2^+	δ_{KMT}	0.477	935	250	70	18	27
(3.90 MeV)	δ_{RIA}	0.392	84	52	6	27	10
	$\delta_{RIA\text{-}SE}$	0.388	84	53	7	27	9
5^-	δ_{KMT}	0.975	942	251	71	1414	336
(4.49 MeV)	δ_{RIA}	0.833	80	48	5	300	97
	$\delta_{RIA\text{-}SE}$	0.807	79	55	7	246	70

scattering data is not surprising in view of the failure of this simplified form of the KMT to reproduce the elastic spin observables. The results shown in Figs. 1–4 illustrate this point where KMT and RIA calculations are compared to the data.[20–22] Just as in the RIA case there are ambiguities when the number of parameters is increased beyond three.

The RIA and first-order KMT predictions for elastic scattering are shown in Figs. 1 and 2 in comparison with the data.[20] Channel coupling to the 3^-,3.74 MeV state was included in both calculations. The very good description of the data provided by the RIA model (solid curves) is essentially the same as that shown in Ref. 1. The forward angle predictions of the first-order KMT model (dashed curves) are consistent with that shown elsewhere.[3,4] At large angles greater than $30^\circ_{c.m.}$ the diffractive structure in the KMT predictions is shifted outward relative to similar calculations given in the second paper cited in Ref. 20, which do not include channel coupling. For example, the angular positions of the predicted and measured diffractive minima in the differential cross section shown in Fig. 1 agree (particularly for the minimum near $38^\circ_{c.m.}$) whereas they do not in the uncoupled KMT predictions. However the predicted minima are too deep and the overall magnitude of the predicted differential cross section decreases too rapidly with increasing scattering angle. The large angle KMT A_y predictions qualitatively describe the data but do not provide as good a description as the RIA.

The values of the deformation lengths obtained in the searches are given in Tables I and II. The RIA values obtained in the one parameter searches, which produce the observables shown in Figs. 1–4, are in good agreement with previous work.[1] Because the KMT based model produces rather poor agreement with the spin observables, comparison of the resulting δ's with the RIA δ's is meaningless. If we allow the central and spin-orbit deformation lengths to be free parameters in the KMT calculation we find that $\delta_{s.o.}$ becomes very large and that the agreement with the inelastic spin observables is improved. However, the RIA based model seems clearly superior to the first-order KMT calculation. The RIA re-

TABLE II. The deformation lengths determined from two parameter fits to the 497.5 MeV ^{40}Ca(p,p') data. The KMT or RIA optical potentials were used in the collective model calculations.

State			δ (fm)	$\frac{\chi^2_{e,CS}}{N}$	$\frac{\chi^2_{e,Ay}}{N}$	$\frac{\chi^2_{e,Q}}{N}$	$\frac{\chi^2_{i,CS}}{N}$	$\frac{\chi^2_{i,Ay}}{N}$
3^-	KMT	δ_c	1.044	927	261	80	63	248
(3.74 MeV)		$\delta_{s.o.}$	2.601					
	RIA	δ_s	1.154	89	56	8	57	14
		δ_v	1.219					
2^+	KMT	δ_c	0.547	932	252	72	17	6
(3.90 MeV)		$\delta_{s.o.}$	0.227					
	RIA	δ_s	0.331	84	53	7	30	1.3
		δ_v	0.350					
5^-	KMT	δ_c	0.215	1015	252	74	191	46
(4.49 MeV)		$\delta_{s.o.}$	1.587					
	RIA	δ_s	0.582	80	53	7	219	40
		δ_v	0.668					

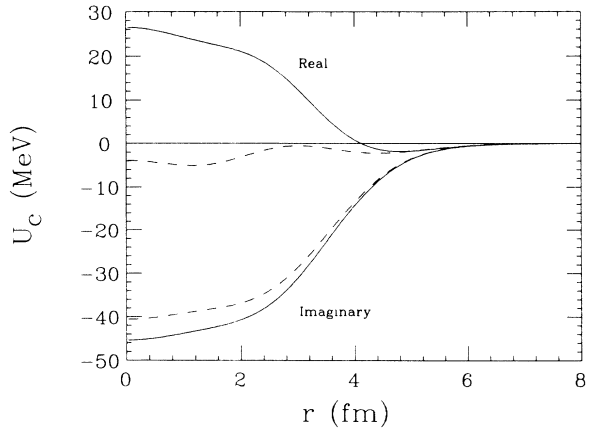

FIG. 5. The central potentials for the KMT (dashed line) and RIA-SE (solid line) calculations.

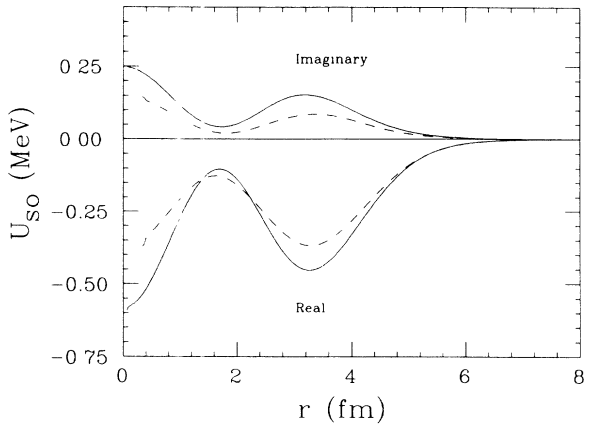

FIG. 6. The spin-orbit potentials for the KMT (dashed line) and RIA-SE (solid line) calculations.

sults are quite similar to phenomenological work[11] and with the work of Hicks and Lisantti[23] who compare Dirac model predictions with a nonrelativistic model using Love-Franey[24] *NN* amplitudes in the nonrelativistic impulse approximation optical potentials.

Next we address the question regarding the necessity of using coupled channel Dirac equations. In order to accomplish this we use a diagonal potential in the Schrödinger calculation which produces agreement with the elastic observables. This potential, shown in Figs. 5 and 6, results from the reduction of the Dirac equation to second order form.[25,26] The potentials, usually termed the "Schrödinger equivalent" (SE) central and spin-orbit potentials, were used as input to the Schrödinger coupled channel calculation using the same δ for the central and spin-orbit terms. In Figs. 5 and 6 we show both the KMT and RIA-SE central and spin-orbit elastic optical potentials. The results of the analysis using the RIA-SE potentials are given in Table I, and they show that if the elastic data is well reproduced, and the state is collective, then the inelastic data can be well represented regardless of which set of coupled equations is used. Thus, we conclude that using either the Schrödinger or the Dirac coupled equations in the analysis produces almost the same deformation lengths and equally good descriptions of the data. This implies that for this case a reduction of the coupled channel Dirac equations in analogy with that often done for the elastic channel would result in diagonal and coupling potentials that are essentially the same as the "Schrödinger equivalent" potentials.

III. CONCLUSIONS

We have compared the results of relativistic and nonrelativistic coupled channel calculations for elastic and inelastic $p+{}^{40}$Ca scattering observables at 500 MeV. The diagonal potentials were obtained from either the first-order KMT impulse approximation or the RIA prescription. The off-diagonal potentials were calculated from these elastic channel optical potentials using a simple collective model approach. We found that the RIA predictions were superior to those of this simplified version of the KMT with respect to reproducing the elastic data at forward and large angles as well as inelastic spin observables. Neither calculation contains Pauli blocking or other medium effects which tend to improve the nonrelativistic model predictions for the elastic scattering.[27]

We have also shown that the use of coupled channel Dirac equations is not a necessary requirement for reproducing these inelastic data. Finally, we demonstrated that the failure of the first-order KMT impulse approximation collective model to describe the inelastic scattering data is due to the fact that the transition potential is generated from the elastic channel optical potential which itself fails to reproduce the elastic scattering data.

This work was supported in part by the National Science Foundation, under Grant No. Phy-8822550 and the U.S. Department of Energy.

[1]S. Shim, B. C. Clark, S. Hama, E. D. Cooper, R. L. Mercer, L. Ray, and G. W. Hoffmann, Phys. Rev. C **38**, 1968 (1988).

[2]J. A. McNeil, J. R. Shepard, and S. J. Wallace, Phys. Rev. Lett. **50**, 1439 (1983); J. R. Shepard, J. A. McNeil, and S. J. Wallace, *ibid.* **50**, 1443 (1983).

[3]B. C. Clark, S. Hama, R. L. Mercer, L. Ray, and B. D. Serot, Phys. Rev. Lett. **50**, 1644 (1983); B. C. Clark, S. Hama, R. L. Mercer, L. Ray, G. W. Hoffmann, and B. D. Serot, Phys. Rev. C **28**, 1421 (1983).

[4]L. Ray and G. W. Hoffmann, Phys. Rev. C **31**, 538 (1985); **34**, 2353(E) (1986).

[5]M. V. Hynes, A. Picklesimer, P. C. Tandy, and R. M. Thaler, Phys. Rev. Lett. **52**, 978 (1984); Phys. Rev. C **31**, 1438 (1985).

[6]A. K. Kerman, H. McManus, and R. M. Thaler, Ann. Phys. (N.Y.) **8**, 551 (1959).

[7]G. W. Hoffmann, L. Ray, M. L. Barlett, R. Fergerson, J.

McGill, E. C. Milner, K. K. Seth, D. Barlow, M. Bosko, S. Iverson, M. Kaletka, A. Saha, and D. Smith, Phys. Rev. Lett. **47**, 1436 (1981).

[8]R. A. Arndt, J. S. Hyslop, and L. D. Roper, Phys. Rev. D **35**, 128 (1987); R. A. Arndt, L. D. Roper, R. A. Bryan, R. B. Clark, B. J. Ver West, and P. Signell, Phys. Rev. D **28**, 97 (1983).

[9]J. A. McNeil, L. Ray, and S. J. Wallace, Phys. Rev. C **27**, 2123 (1983).

[10]C. J. Horowitz and B. D. Serot, Nucl. Phys. A **368**, 503 (1981).

[11]S. Shim, Ph.D. thesis, Ohio State University, 1989 (unpublished).

[12]J. Raynal, H. S. Sherif, A. M. Kobos, E. D. Cooper, and J. I. Johansson, Phys. Lett. B **218**, 403 (1989).

[13]R. L. Mercer, Phys. Rev. C **15**, 1786 (1977); R. L. Mercer and D. G. Ravenhall, *ibid.* **10**, 2002 (1974); R. L. Mercer, Ph.D. thesis, University of Illinois, 1972 (unpublished).

[14]W. Rory Coker and L. Ray, Phys. Rev. C **42**, 659 (1990).

[15]H. S. Sherif and J. S. Blair, Phys. Lett. **26B**, 489 (1968).

[16]Taro Tamura, Rev. Mod. Phys. **37**, 679 (1965).

[17]J. Raynal, in *The Proceedings of the Workshop on Applied Theory and Nuclear Model Calculations for Nuclear Technology Applications,* ICTP Trieste, 1988 (World Scientific, Singapore, 1989); Phys. Lett. B **196**, 7 (1987).

[18]E. D. Cooper, Ph.D. thesis, University of Alberta, 1981 (unpublished).

[19]L. Ray, Phys. Rev. C **19**, 1855 (1979).

[20]The elastic differential cross section and analyzing power data for angles less than 30° are from G. W. Hoffmann *et al.*, Phys. Rev. Lett. **47**, 1436 (1981); the larger angle data are from G. W. Hoffmann *et al.*, Phys. Rev. C **37**, 1307 (1988); and the elastic spin rotation data are from A. Rahbar *et al.*, Phys. Rev. Lett. **47**, 1811 (1981).

[21]K. Seth, D. Barlow, A. Saha, R. Soundranayagam, S. Iversen, M. Kaletka, M. Basko, D. Smith, G. W. Hoffmann, M. L. Barlett, R. Fergerson, J. McGill, and E. C. Milner, Phys. Lett. **158B**, 23 (1985).

[22]M. L. Barlett, G. W. Hoffmann, and L. Ray, Phys. Rev. C **35**, 2185 (1987).

[23]K. H. Hicks and J. Lisantti, Nucl. Phys. **A484**, 432 (1988).

[24]M. A. Franey and W. G. Love, Phys. Rev. C **31**, 488 (1985).

[25]B. C. Clark, S. Hama, and R. L. Mercer, in *The Proceedings of the Workshop on the Interaction Between Medium Energy Nucleons in Nuclei* (Indiana University Cyclotron Facility, Bloomington, Indiana), AIP Conf. Proc. No. 97, edited by H. O. Meyer (AIP, New York, 1982), p. 260.

[26]S. Hama, B. C. Clark, E. D. Cooper, H. S. Sherif, and R. L. Mercer, Phys. Rev. C **41**, 2737 (1990).

[27]L. Ray, Phys. Rev. C **41**, 2816 (1990).